Critical behavior of double perovskite La_2NiMnO_6

2008 J. Phys.: Condens. Matter 20 465211

(http://iopscience.iop.org/0953-8984/20/46/465211)

J. Phys.: Condens. Matter **20** (2008) 465211 (5pp) doi:10.1088/0953-8984/20/46/465211

Critical behavior of double perovskite La_2NiMnO_6

X Luo, B Wang, Y P Sun[1], X B Zhu and W H Song

Key Laboratory of Materials Physics, Institute of Solid State Physics, and High Magnetic Field Laboratory, Chinese Academy of Sciences, Hefei 230031, People's Republic of China

E-mail: ypsun@issp.ac.cn

Received 12 March 2008, in final form 8 September 2008
Published 21 October 2008
Online at stacks.iop.org/JPhysCM/20/465211

Abstract

The critical behavior of the double perovskite La_2NiMnO_6 was investigated by measurement of the magnetization around the Curie temperature T_C. The magnetic data were analyzed in the critical region using the Kouvel–Fisher method to yield the critical exponents of $\beta = 0.408 \pm 0.011$ with $T_C = 270.50$ (from the temperature dependence of the spontaneous magnetization below T_C) and $\gamma = 1.295 \pm 0.015$ with $T_C = 271.10$ (from the temperature dependence of the inverse initial susceptibility above T_C). The critical magnetization isotherm $M(T_C, H)$ gives $\delta = 4.139 \pm 0.090$. The critical exponents obtained by this method obey the Widom scaling relation $\delta = 1 + \gamma/\beta$, implying the critical exponents are reliable. The values of critical exponents are close to those predicted by the three-dimensional (3D) Heisenberg model with short-range interactions.

(Some figures in this article are in colour only in the electronic version)

1. Introduction

The colossal magnetoresistance (CMR) effect in perovskite manganese oxides $R_{1-x}A_xMnO_3$ (R = rare-earth ions; A = divalent ions) has attracted much research attention in recent years [1–3]. The close relation between transport and magnetism in these materials has been explained by the double exchange (DE) mechanism, where the e_g electrons of Mn^{3+} hop between neighboring sites via the 2p orbital of O^{2-} [4], phase separation combined with percolation [5] and so on, but the physical mechanism of the CMR effect remains controversial. To better understand the metal–insulator transition and the CMR effect, it is essential to fully study the nature of the paramagnetic (PM)–ferromagnetic (FM) transition. One of the effective methods is to study in detail the critical exponents associated with the transition. Many experimental studies of critical behavior have been made on some manganites [6–14] and the half-metal double perovskite oxide Sr_2FeMoO_6 [15]. The values of the critical exponent β obtained from a variety of techniques range from 0.3 to 0.5. For example, the β value reported for the $La_{0.7}Sr_{0.3}MnO_3$ single crystal is close to that of the 3D Heisenberg model [5]. In the series of compounds $La_{1-x}Ca_xMnO_3$, there exists a tricritical point at $x = 0.4$ that sets a boundary between first-order ($x < 0.4$) and second-order ($x > 0.4$) FM phase transitions in the FM range ($0.2 < x < 0.5$) [8]. Thus, the critical exponents can supply some useful information about the PM–FM transition.

La_2NiMnO_6 is an FM semiconductor and one of the most promising materials for spintronic devices. La_2NiMnO_6 crystallizes in an ordered double perovskite with a pseudocubic structure. NiO_6 and MnO_6 octahedra are ordered in a rock-salt configuration in the pseudocubic structure [16, 17]. Its PM–FM transition temperature (Curie temperature T_C) is about 280 K. The magnetic properties of La_2NiMnO_6 can be well explained by Kanamori–Goodenough rules. However, disagreements exist about the cation oxidation state (i.e. Ni^{2+}/Mn^{4+} or Ni^{3+}/Mn^{3+}) and the Ni/Mn ordering in the B-site sublattice. Although some experimental results, such as ^{55}Mn NMR and x-ray absorption spectroscopy [18–20], have provided evidence for ordered Mn^{4+}–O–Ni^{2+} superexchange interactions in La_2NiMnO_6, the two results of neutron diffraction disagree about the manganese and nickel oxidation states. Blasco *et al* report that the neutron diffraction refinements for the La_2NiMnO_6 support the presence of Ni^{2+} and Mn^{4+} [21], whereas Bull and coworkers conclude that Ni^{3+} and Mn^{3+} are present [22]. Thus, it is clear that the nature of the magnetic transition in La_2NiMnO_6 is not fully

[1] Author to whom any correspondence should be addressed.

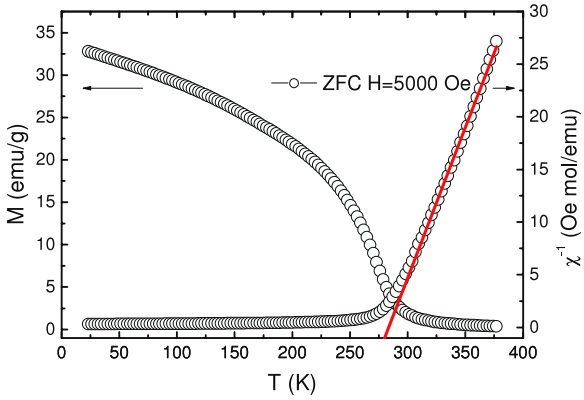

Figure 1. Temperature dependence of magnetization and the inverse of magnetic susceptibility measured at $H = 5000$ Oe in the zero-field-cooling mode for La_2NiMnO_6. The inset shows the plot of dM/dT as a function of temperature at $H = 5000$ Oe.

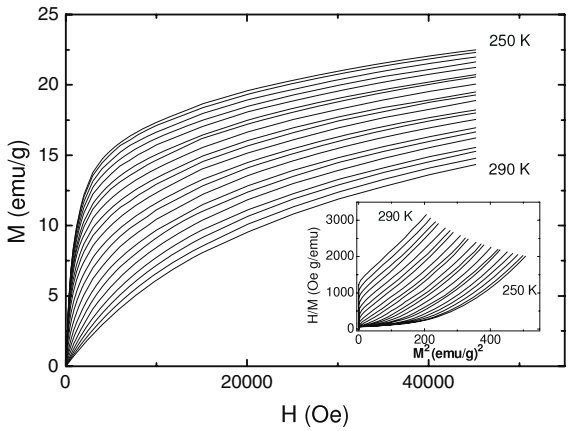

Figure 2. M versus H of La_2NiMnO_6 between 250 and 290 K (in 2 K steps). The inset shows Arrott plots of H/M versus M^2. The positive slope indicates a second-order transition.

understood yet. As mentioned above, the critical exponents usually provide some useful extra information about the nature of the PM–FM transition of materials. Therefore, in order to understand better the nature of the magnetic transition in La_2NiMnO_6, we perform the investigation of the critical behavior of La_2NiMnO_6 in this paper.

2. Experimental details

La_2NiMnO_6 samples with nanoscale grains were prepared by the citrate gel technique. The detailed preparation procedure can be found in many places [23, 24]. The metal nitrates mixed in stoichiometric composition were dissolved together in water, and the ethylene glycol was also added to make a solution complex. The solution was evaporated and dried at 473 K and preheated at 873 K to remove the remaining organic solvent and decompose the nitrates of the gel. The final powders were ground, pelletized and sintered at 1373 K for 24 h and cooled slowly to room temperature. The phase purity was examined by powder x-ray diffraction using Cu Kα radiation at room temperature. The sample was found to have a perovskite structure, and the lattice parameters were in agreement with those reported in the literature [16]. The magnetic measurements were carried out with a Quantum Design superconducting quantum interference device (SQUID) magnetic properties measurement system ($1.8\ \text{K} \leqslant T \leqslant 400\ \text{K}$, $0\ \text{T} \leqslant H \leqslant 5\ \text{T}$). The measured samples are considered as cylinders, with length 6 mm and diameter 1 mm, and the applied field is parallel to the longest semiaxis of the samples. So the field can exist throughout the samples and the shape demagnetizing fields can be reduced as much as possible.

3. Results and discussion

Figure 1 shows the temperature dependence of the magnetization $M(T)$ under the zero-field-cooling mode at an applied field of 5000 Oe. The Curie temperature T_C (defined as the one corresponding to the peak of dM/dT in M versus T) is 276 K, which is characteristic of an atomically ordered Ni^{2+} and Mn^{4+}. The $M(T)$ can be well fitted by the Curie–Wiess law $\chi(T) = C/(T - \theta_p)$ at high temperature and the parameters of $C = 3.51\ \text{K cm}^3\ \text{mol}^{-1}$ ($\mu_{\text{eff}} = 5.28\ \mu_B$) and $\theta_p = 280$ K are obtained, which are in agreement with reported values [16, 23].

According to the scaling hypothesis, the second-order magnetic phase transition near the Curie point is characterized by a set of critical exponents, α, β, γ, δ, etc, and a magnetic equation of state [25]. The exponent α can be obtained from the specific heat and β and γ from spontaneous magnetization and initial susceptibility, below and above T_C, respectively, while δ is the critical isotherm exponent. Those exponents from magnetization measurements are given below:

$$M_S(T) = M_0|\varepsilon|^{-\beta}, \qquad \varepsilon < 0, \quad T < T_C \tag{1}$$

$$\chi_0^{-1}(T) = (h_0/M_0)\varepsilon^{\gamma}, \qquad \varepsilon > 0, \quad T > T_C \tag{2}$$

$$M = DH^{1/\delta}, \qquad \varepsilon = 0, \quad T = T_C \tag{3}$$

where $\varepsilon = (T - T_C)/T_C$ is the reduced temperature, and M_0, h_0/M_0 and D are the critical amplitudes.

The magnetic equation of state in the critical region is written as

$$M(H, \varepsilon) = \varepsilon^{\beta} f_{\pm}(H/\varepsilon^{\beta+\gamma}), \tag{4}$$

where f_+ for $T > T_C$ and f_- for $T < T_C$, respectively, are regular functions. Equation (4) implies that the $M|\varepsilon|^{-\beta}$ as a function of $H|\varepsilon|^{-\beta+\gamma}$ produces two universal curves: one for temperatures below T_C and the other for temperatures above T_C.

Figure 2 shows a series of isotherms of magnetization M versus H in the temperature range $T_C \pm 20$ K. The inset shows a plot of H/M versus M^2 with positive slopes indicating a second-order phase transition [26, 27].

Figures 3(a) and (b) show the modified Arrott plots at different temperatures modified by using the critical exponents of the mean-field model and of the three-dimensional (3D) Heisenberg model. According to the mean-field theory near T_C, M^2 versus H/M at various temperatures should show a series of parallel lines and the line at $T = T_C$ has to pass

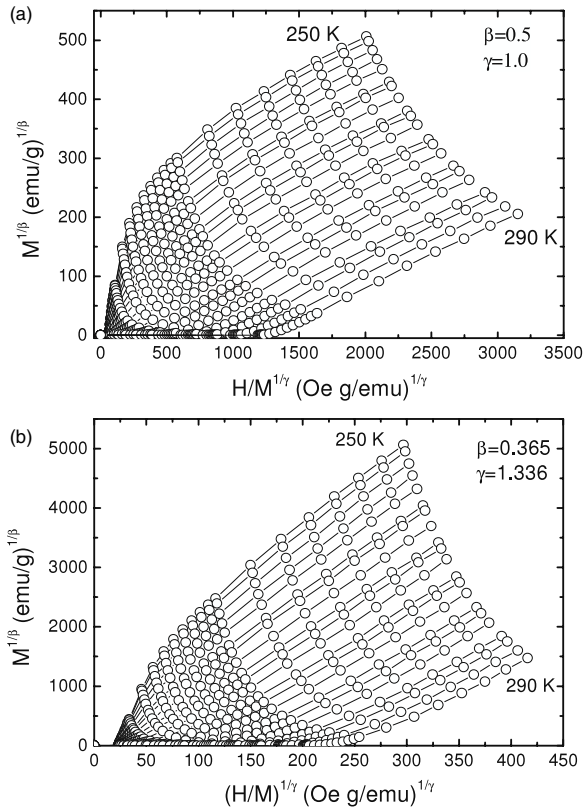

Figure 3. (a) Isotherms of M^2 versus H/M at different temperatures around T_C. (b) Modified Arrott plots $M^{1/\beta}$ versus $(H/M)^{1/\gamma}$ in the case of the 3D Heisenberg model ($\beta = 0.365$ and $\gamma = 1.336$).

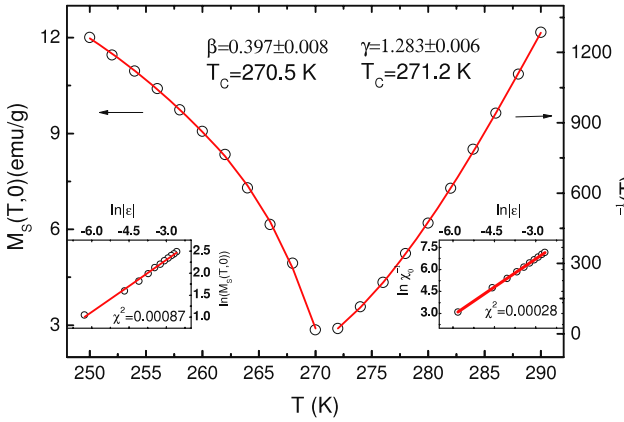

Figure 4. Temperature dependence of the spontaneous magnetization $M_S(T, 0)$ and the inverse initial susceptibility $1/\chi_0(T)$. The inset reproduces a double logarithmic plot of $M_S(T, 0)$ and $1/\chi_0(T)$ versus reduced temperature $\varepsilon = (T - T_C)/T_C$ (using T_C shown in the plot) along with equations (1) and (2).Those slopes yield the values of the exponents β and γ shown. The parameter χ^2 stands for the quality of the fit.

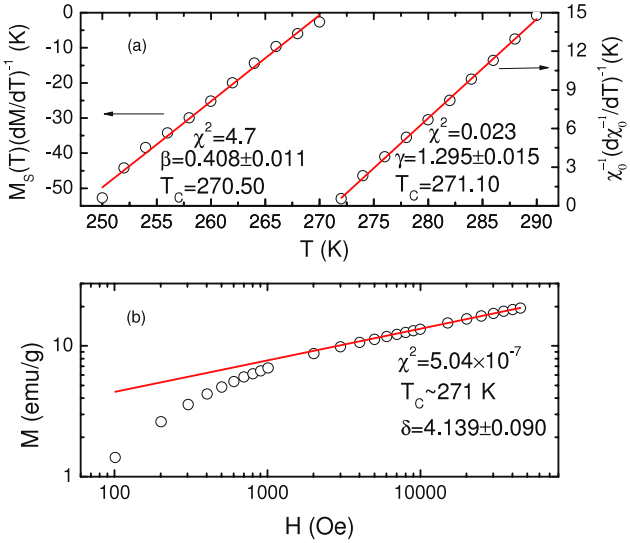

Figure 5. (a) Kouvel–Fisher plots for the spontaneous magnetization and the inverse initial susceptibility. (b) Critical isotherms on a log–log scale for La_2NiMnO_6 at $T_C \sim 271$ K. The parameter χ^2 denotes the quality of the fit.

through the origin. In our sample, the curves in the Arrott plots are not linear, implying that the mean-field model is not valid for La_2NiMnO_6. As trial values, we have chosen the critical exponents of the 3D Heisenberg model ($\beta = 0.365$, $\gamma = 1.336$). The isotherms are almost parallel straight lines at higher fields. From the Arrott plots in figure 2(a), the curves below and above T_C can be extended smoothly into the H/M axis to yield reliable values of the $M_S(T, 0)$ and $1/\chi_0(T)$. The polynomial fit is also performed and extrapolation of the data for $T < T_C$ gives reliable values of $M_S(T, 0)$ from $H = 0.5$ to 4.5 T [28].

$M_S(T, 0)$ versus T and $1/\chi_0(T)$ versus T are plotted in figure 4. The insets show these same data replotted against the reduced temperature $\varepsilon = (T - T_C)/T_C$, using $T_C = 270.5$ and 271.2 K, on a log–log scale; these insets confirm directly the power-law predictions of equations (1) and (2), respectively. The critical exponents were determined to be $\beta = 0.397 \pm 0.008$ and $\gamma = 1.283 \pm 0.006$. In addition, the critical exponents were also obtained by the Kouvel–Fisher (KF) method [29]:

$$M_S(T)[\mathrm{d}M_S(T)/\mathrm{d}T]^{-1} = (T - T_C)/\beta, \tag{5}$$

$$\chi_0^{-1}(T)[\mathrm{d}\chi_0^{-1}(T)/\mathrm{d}T]^{-1} = (T - T_C)/\gamma. \tag{6}$$

According to these equations, plots of $M_S(T)[\mathrm{d}M_S(T)/\mathrm{d}T]^{-1}$ versus T and $\chi_0^{-1}(T)[\mathrm{d}\chi_0^{-1}(T)/\mathrm{d}T]^{-1}$ versus T should yield straight lines with slopes $1/\beta$ and $1/\gamma$, respectively, and the intercepts on the T axes equal to T_C. The results are shown in figure 5(a). It shows that the lines from the KF method are approximately linear, which suggests that the errors of the measurement can be nearly ignored and our derived values of $M_S(T, 0)$ and $1/\chi_0(T)$ are reliable. We obtain the critical exponents $\beta = 0.408 \pm 0.011$ with $T_C = 270.50$ and $\gamma = 1.295 \pm 0.015$ with $T_C = 271.10$. In figure 5(b), the critical isotherms M versus H are plotted on a log–log scale. The critical temperature is 270 K, which is close to the T_C. According to equation (3), this should be a straight line in the high-field region with the slope $1/\delta$. This gives the δ value of 4.139 ± 0.090. The critical exponents from this static scaling

Table 1. Comparison of critical parameters of La_2NiMnO_6 with different theoretical models, the conventional ferromagnet Ni, the half-metal double perovskite oxide Sr_2FeMoO_6 and some manganites reported in the literature. Abbreviations: SC, single crystal; PC, polycrystalline; NS, not specified.

Material	Reference	T_C (K)	β	γ	δ
La_2NiMnO_6	This work	270.80	0.408 ± 0.011	1.295 ± 0.015	4.139 ± 0.090
Mean-field model	[25]		0.5	1.0	3.0
3D Heisenberg model	[25]		0.365 ± 0.003	1.336 ± 0.004	4.80 ± 0.04
3D Ising model	[25]		0.325 ± 0.002	1.241 ± 0.002	4.82 ± 0.02
Ni	[25]	627.4	0.378 ± 0.004	1.34 ± 0.01	4.58 ± 0.04
Sr_2FeMoO_6 (SC)	[15]	409.1	0.388 ± 0.004	1.30 ± 0.01	4.35
$La_{0.7}Sr_{0.3}MnO_3$ (SC)	[6]	354.0 ± 0.2	0.37 ± 0.04	1.22 ± 0.03	4.25 ± 0.2
$La_{0.75}Sr_{0.25}MnO_3$ (SC)	[7]	346	0.40 ± 0.02	1.27 ± 0.06	4.12 ± 0.33
$La_{0.875}Sr_{0.125}MnO_3$ (SC)	[8]	186.1	0.37 ± 0.02	1.38 ± 0.03	4.72 ± 0.04
$La_{0.6}Ca_{0.4}MnO_3$ (PC)	[9]	265.5	0.25 ± 0.03	1.03 ± 0.05	5.0 ± 0.8
$La_{0.7}Ca_{0.3}MnO_3$ (SC)	[10]	222 ± 0.2	0.14 ± 0.02	0.81 ± 0.03	1.22 ± 0.02
$La_{0.5}Sr_{0.5}CoO_3$ (PC)	[11]	223	0.321 ± 0.002	1.351 ± 0.009	4.39 ± 0.02
$La_{0.67}Ba_{0.33}MnO_3$ (PC)	[12]	306.1 ± 0.2	0.356 ± 0.004	1.12 ± 0.03	NS
$Nd_{0.6}Pb_{0.4}MnO_3$ (SC)	[13]	156.47 ± 0.06	0.374 ± 0.006	1.329 ± 0.003	4.54 ± 0.10
$Pr_{0.77}Pb_{0.23}MnO_3$ (SC)	[14]	167.02 ± 0.04	0.344 ± 0.001	1.352 ± 0.006	4.69 ± 0.02

analysis are related to the Widom scaling relation [30]

$$\delta = 1 + \gamma/\beta. \tag{7}$$

Using the above scaling relation and estimated values of β and γ from the KF method, we obtain $\delta = 4.174 \pm 0.005$. The result obtained from the scaling relation is close to the estimated $\delta = 4.139 \pm 0.090$ value from the critical isotherms at 271 K, which is close to T_C. Thus, the critical exponents found in the KF method obey the Widom scaling relation. The critical exponents obtained by the magnetization data are reliable and in agreement with the scaling hypothesis.

In order to check whether our data in the critical region obey the magnetic equation of state as described by equation (4), $M|\varepsilon|^{-\beta}$ as a function of $H|\varepsilon|^{-\beta+\gamma}$ is plotted in figure 6 using the values of critical exponents obtained from the KF method and $T_C \sim 271$ K. The inset shows the same results on a log–log scale. All the points fall on two curves, one for $T < T_C$ and the other for $T > T_C$. This suggests that the value of the exponents and T_C are reasonably accurate.

The values of the critical exponents of La_2NiMnO_6 (present work), the theoretical values based on various models, the conventional ferromagnet Ni, the half-metallic double perovskite oxide Sr_2FeMoO_6 and other manganites present in the literature are listed in table 1 for comparison. Obviously, the critical exponents of the La_2NiMnO_6 obtained from the magnetic data are between the mean-field model and the 3D Heisenberg model values. The data in table 1 support the conclusion that the critical exponents of some manganites [6–14] and the half-metal double perovskite oxide Sr_2FeMoO_6 [15] belong to the universality class of a 3D isotropic Heisenberg ferromagnet with short-range couplings. The following information is also obtained from table 1: the critical exponents are governed by the lattice dimension ($D = 3$, in the present case), the dimension of order parameter ($n = 3$, magnetization) and the range of interaction (short range, long range or infinite) [31]. In homogeneous magnets the universality class of the magnetic phase transition depends on the range of the exchange interaction $J(r) = 1/r^{d+\sigma}$, where d is the dimension of the system and σ is the range of

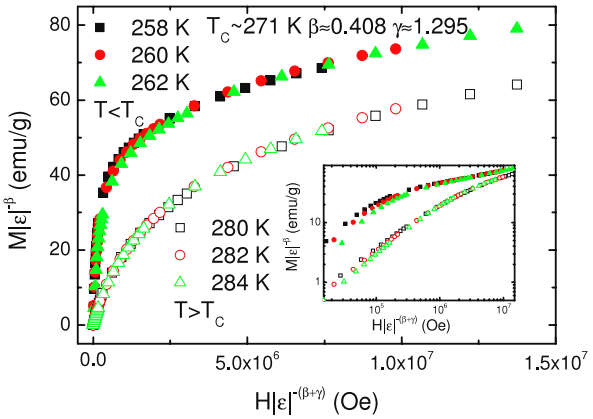

Figure 6. Scaling plots for La_2NiMnO_6 below and above T_C using β and γ determined by the Kouvel–Fisher method. The inset shows the same plots on a log–log scale.

interaction [31]. It has been argued that, if σ is greater than 2, the 3D Heisenberg exponents ($\beta = 0.365$, $\gamma = 1.336$, $\delta = 4.8$) are valid. The mean-field exponents ($\beta = 0.5$, $\gamma = 1$, $\delta = 3$) are valid for σ less than 3/2. For the intermediate range, $3/2 < \sigma < 2$, the exponents belong to different universality classes which depend on σ. In the case of the double perovskite oxide La_2NiMnO_6, the γ value is close to the isostructural oxide Sr_2FeMoO_6, which is a 3D Heisenberg ferromagnet. However, the β value is between the predicted value of the mean-field model and the 3D Heisenberg model and close to that of the 3D Heisenberg model shown in table 1. This difference is suggested to originate from the β value calculated from fittings below T_C, whereas γ is from above T_C [27]. A crossover to another universality class due to magnetic anisotropy should be unobservable in our studied polycrystalline sample [32].

The ferromagnetism of the La_2NiMnO_6 is affected by the short-range interaction related to the strong spin–phonon coupling above the T_C in La_2NiMnO_6 [33–35]. First-principles density functional calculations also show the presence of strong coupling between the spins and phonons [36]. That

to say, the short-range interaction induced by the spin–phonon coupling has the key impact on the ferromagnetism of the La_2NiMnO_6. However, from the results as shown in figure 3(b), i.e. $M^{1/\beta}$ versus $(H/M)^{1/\gamma}$ according to the 3D Heisenberg model ($\beta = 0.365$ and $\gamma = 1.336$) the plots exhibit nearly linear isothermal curves in the higher field, and using the values of the critical exponents obtained from the KF method we find that all points of the magnetization fall on two curves responding to below and above T_C as shown in figure 6. The results are consistent with the above related experimental and calculated results. Therefore, the conclusion that the double perovskite oxide La_2NiMnO_6 might be a 3D Heisenberg ferromagnetic with short-range interactions can be obtained. In order to make sure of the explicit universality class of La_2NiMnO_6, a high purity single crystal is required for its critical research.

4. Conclusion

In summary, we have used magnetization measurements to study the critical properties of the double perovskite oxide La_2NiMnO_6 at temperatures around T_C. The critical exponents of $\beta = 0.408\pm0.011$ with $T_C = 270.50$ and $\gamma = 1.295\pm0.015$ with $T_C = 271.10$ were determined by using the KF method. The value of δ was 4.139 ± 0.090, obtained from the critical isotherm $M(T_C, H)$. The critical exponents of La_2NiMnO_6 were between those predicted by the mean-field model and the 3D Heisenberg model and close to those predicted by the 3D Heisenberg model, which suggests that La_2NiMnO_6 might be a 3D Heisenberg ferromagnet with short-range interactions.

Acknowledgments

This work was supported by the National Key Basic Research under contract no. 2007CB925002, the National Science Foundation of China under contract nos. 10774146 and 50672099, and the Director's Fund of the Hefei Institutes of Physical Science, Chinese Academy of Science.

References

[1] Jim S, Tiefel T H, McCormack M, Fastnacht R A, Ramesh R and Chen L H 1994 *Science* **264** 413
[2] von Helmolt R, Wecker J, Holzapfel B, Schultz L and Samwer K 1993 *Phys. Rev. Lett.* **71** 2331
[3] Tokura Y 2000 *Colossal Magnetoresistance Oxides* (New York: Gordon and Breach)
[4] Zener C 1951 *Phys. Rev.* **82** 403
Anderson P W and Hasegawa H 1955 *Phys. Rev.* **100** 675
[5] Mori S, Chen C H and Cheong S-W 1998 *Phys. Rev. Lett.* **81** 3972
[6] Ghosh K, Lobb C J, Greene R L, Karabashev S G, Shulyatev D A, Arsenov A A and Mukovskii Y 1998 *Phys. Rev. Lett.* **81** 4740
[7] Kim D, Zink B L, Hellman F and Coey J M D 2002 *Phys. Rev.* B **65** 214424
[8] Nair S, Banerjee A, Narlikar A V, Prabhakaran D and Boothroyd A T 2003 *Phys. Rev.* B **68** 132404
[9] Kim D, Revaz B, Zink B L, Hellman F, Rhyne J J and Mitchell J F 2002 *Phys. Rev. Lett.* **89** 227202
[10] Shin H S, Lee J E, Nam Y S, Ju H L and Park C W 2001 *Solid State Commun.* **118** 377
[11] Mukherjee S, Raychaudhuri P and Nigam A K 2000 *Phys. Rev.* B **61** 8651
[12] Moutis N, Panagiotopoulos I, Pissas M and Niarchos D 1999 *Phys. Rev.* B **59** 1129
[13] Sahana M, Rössler U K, Ghosh N, Elizabeth S, Bhat H L, Dörr K, Eckert D, Wolf M and Müller K H 2003 *Phys. Rev.* B **68** 144408
[14] Padmanabhan B, Bhat H L, Elizabeth S, Röszler S, Röszler U K, Dörr K and Müller K H 2007 *Phys. Rev.* B **75** 024419
[15] Yanagihara H, Cheong W, Salamon M B, Xu Sh and Moritomo Y 2002 *Phys. Rev.* B **65** 092411
[16] Dass R I, Yan J Q and Goodenough J B 2003 *Phys. Rev.* B **68** 064415
[17] Goodenough J B, Wold A, Arnott R J and Menyuk N 1961 *Phys. Rev.* **124** 373
[18] Asai K, Sekizawa H and Iida S 1979 *J. Phys. Soc. Japan* **47** 1054
[19] Sonobe M and Asai K 1992 *J. Phys. Soc. Japan* **61** 4193
[20] Sanchez M C, Garcia J, Blasco J, Subias G and Perez-Cacho J 2002 *Phys. Rev.* B **65** 144409
[21] Blasco J, Sanchez M C, Perez-Cacho J, Garcia J, Subias G and Campo J 2002 *J. Phys. Chem. Solids* **63** 781
[22] Bull C L, Gleeson D and Knight K S 2003 *J. Phys.: Condens. Matter* **15** 4972
[23] Rogada N S, Li J, Sleight A W and Subramanian M A 2005 *Adv. Mater. (Weinheim)* **17** 2225
[24] Yang J, Ma Y Q, Zhang R L, Zhao B C, Ang R, Song W H and Sun Y P 2005 *Solid State Commun.* **136** 268
[25] Stanley H E 1971 *Introduction to Phase Transition and Critical Phenomena* (Oxford: Oxford University Press)
[26] Banerjee S K 1964 *Phys. Lett.* **12** 16
[27] Mira J, Rivas J, Rivadulla F, Vázquez-Vázquez C and López-Quintela M A 1999 *Phys. Rev.* B **60** 2998
[28] Yang J, Lee Y P and Li Y 2007 *Phys. Rev.* B **76** 054442
[29] Kouvel J S and Fisher M E 1964 *Phys. Rev.* **136** A1626
[30] Widom B 1964 *J. Chem. Phys.* **41** 1633
Widom B 1965 *J. Chem. Phys.* **43** 3898
[31] Fisher M E, Ma S K and Nickel B G 1972 *Phys. Rev. Lett.* **29** 917
[32] Fisher M E 1974 *Rev. Mod. Phys.* **46** 597
[33] Iliev M N, Guo H and Gupta A 2007 *Appl Phys. Lett.* **90** 151914
[34] Singh M P, Grygiel C, Sheets W C, Boullay Ph, Prellier W, Mercey B, Simon Ch and Raveau B 2007 *Appl. Phys. Lett.* **91** 012506
[35] Zhou S M, Shi L, Yang H P and Zhao J Y 2007 *Appl. Phys. Lett.* **91** 172505
[36] Das H, Waghmare U V, Dasgupta T S and Sarma D D 2008 *Phys. Rev. Lett.* **100** 186402